

Imaging of Submillisecond T_2 Species with 2D and 3D Radial Imaging Sequences

A. Techawiboonwong¹, H. Song¹, and F. W. Wehrli¹

¹Laboratory for Structural NMR Imaging, Department of Radiology, University of Pennsylvania School of Medicine, Philadelphia, Pennsylvania, United States

Introduction

Short- T_2 water protons such as those in connective tissue and bone produce no detectable signal with conventional MRI sequences. Special techniques employing short-duration RF pulse in conjunction with center-out radial data sampling, which have been reported previously for in-vivo imaging of bone and fibrous tissue are therefore required [1]. Both spatially selective half-RF pulses [2] and nonselective rectangular pulses have been used to minimize the delay between signal excitation and detection of k-space center. Although both types of pulses are suited for in-vivo imaging of humans, a full analysis of these two excitation schemes has not been reported. Here we have analyzed excitation profiles of the two schemes and their implications on overall SNR in a 2D radial pulse sequence using half-pulses and in an alternative new 3D hybrid-radial variable-TE sequence with slice-encoding based on non-selective hard pulses in conjunction with outer-slice suppression to achieve spatial selectivity along z. Theoretical excitation profiles were calculated from Bloch equation simulations and compared to the experimental results. Finally, the performance of the two pulse sequences is demonstrated in-vivo in human cortical bone.

Materials and Methods

A radial pulse sequence was designed using the Siemens IDEA pulse sequence editor allowing for both 2D and 3D imaging (Fig. 1). The 2D sequence (a) employs a 560 μ s total duration truncated two-sidlobe half-*sinc* pulse [2] terminated at its peak with the variable-rate selective excitation (VERSE) principle [3] applied during slice-select gradient down-ramp to allow both events to end simultaneously thus eliminating the need for gradient rephasing. The signals from the two excitations with opposed slice-select gradient polarity were combined with real components adding and undesired imaginary components canceling. The 3D sequence (b) employs a 100 μ s rectangular pulse with radial encoding in-plane and phase-encoding in z direction. To reduce the duration between the peak of the excitation and the start of data acquisition (referred to as echo time, TE, even though no real echo is formed) the z-phase encoding gradient was designed for maximum strength and slew rate at each encoding step thus resulting in minimum TE (equal to the receiver dead time) for the $k_z=0$ line and gradually increasing toward k_z^{\max} line [4]. Spatial selectivity along z was accomplished with trains of 1280 μ s dual sidlobe *sinc* outer-volume suppression pulses. Both sequences used radial readout with ramp sampling. In addition, two 5ms rectangular T_2 -selective RF excitation (TELEX [5]) pre-pulses were employed to suppress long- T_2 signals at the frequencies of water and fat protons. Radial data were regridded and reconstructed with standard FT.

The slice profiles and their corresponding images were evaluated in an eraser serving as a homogenous phantom ($T_1=350$ ms, $T_2^*=0.3$ ms). The profiles were obtained with the readout gradients played out in the slice-select direction over two views (at 0° and 180°) with the following parameters: thickness=5mm, TR/flip angle=300ms/65°, TE=0.06ms for half-pulses and 0.11ms for hard pulses, pixel size=0.56mm and read bandwidth=660Hz/pixel. 2D images were acquired with 256 views over 360° for single and three interleaved-slice acquisitions with 20% inter-slice gap. The 3D images were acquired with 256 views over 360° with a 2.5mm slice thickness for 16 slices and TR/flip angle=100ms/41°. Outer-volume suppression over 30mm was achieved by three 12mm partially overlapping saturation slabs positioned at ± 35 , ± 25 and ± 15 mm from the center with 100° flip angle to compensate for T_1 relaxation. Theoretical slice profiles were computed from numerical Bloch equation simulations using the Runge-Kutta 4 method while taking into account relaxation during the RF pulses.

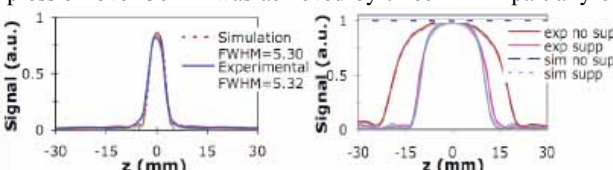


Fig. 2. Half-*sinc* excitation slice profile with a 5mm nominal slice thickness.

Fig. 3. Excitation profile with and without outer-volume suppression normalized to its maximum value.

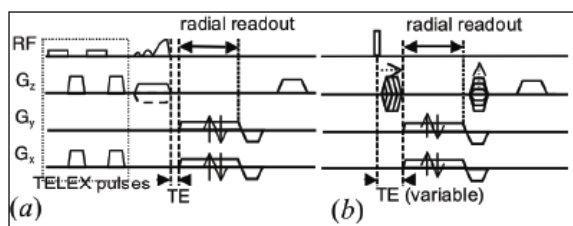


Fig. 1. Radial sequences; (a) 2D radial which utilizes a half-*sinc* pulse and (b) 3D hybrid-radial based on a hard pulse with time-incremented z-encoding gradients. Soft-tissue suppression with TELEX pulses is shown in the dotted box. Both sequences employ readout rewinders followed by a G_z killer gradient.

Images were also obtained in three volunteers (TR/flip angle=300ms/65° (2D) and 70ms/41° (3D), TE=0.05ms (2D) and 0.09-0.23ms (3D), voxel size=0.58x0.58x8mm³, read bandwidth=700Hz/pixel and twenty-three of the 256 samples were collected during the 140 μ s ramping period). 2D scans were obtained in single and multi-slice mode ($N_s=3$, 100% inter-slice gap) with 800 views over 360° in 8 minutes. For 3D images 256 views were collected over 360° with 30 slice encodings (9 mins). All experiments were performed on a 3T Siemens Trio™ system.

Results and Conclusion

Fig. 2 shows the profile of the center slice of the eraser phantom obtained with half-pulse excitation relative to that of the single-slice data. Experimental slice profile integrals averaged over three slices were $86 \pm 9\%$ of the single-slice, in good agreement with predictions ($83 \pm 4\%$). The intensity profile for the 3D excitation with outer-volume suppression is shown in Fig. 3. The outer-volume signals were effectively suppressed, albeit at the expense of signal attenuation in the imaging region (by 23% at the center). Images of the eraser (not shown) yielded relative SNR efficiency of 100.0, 82.3 and 75.2 in the 2d single-, multi-slice and 3D case respectively. 2D and 3D transverse images of the tibial midshaft with soft-tissue suppressions are displayed in Fig. 4. Relative SNR efficiency in solid bone averaged from three subjects were 100.0, 83.1 and 74.5 in the three pulse sequences. Lastly, simulation results showed that when the inequality $\tau_{RF} \ll T_2$ (where τ_{RF} = duration of the RF pulse) is not satisfied, which is the case here even at these short RF pulse durations, some transverse magnetization is lost during nutation. For selective half-pulses and rectangular pulses at the flip angle used this loss is 20% and 8%, respectively, in bone. In conclusion, both pulse sequences perform comparably and effectively capture signal from submillisecond T_2 protons as in cortical bone and fibrous tissues.

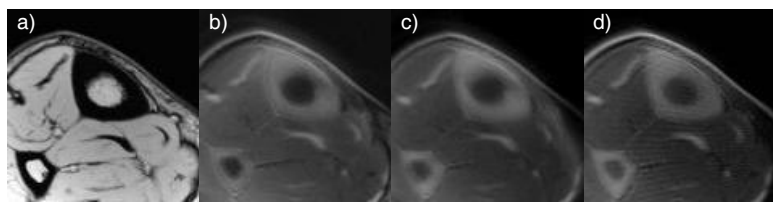


Fig. 4. In-vivo images of tibial midshaft: a) gradient-echo, b)-d) a single-slice 2D, multi-slice 2D and a 3D radial images with soft-tissue signals suppressed. Images highlight signals from bone-water and other connective tissues. SNR of bone is ~ 35 in 8min scan time at $0.58 \times 0.58 \times 8$ mm³ voxel size.

References: 1. Robson MD *et al.*, JCAT 27:825 (2003). 2. Pauly JM *et al.*, Proc.SMRM 8th, 28 (1989). 3. Conolly S *et al.*, JMR 78: 440 (1988). 4. Song HK *et al.*, MRM 39:251 (1998). 5. Sussman MS *et al.*, MRM 40:890 (1998).

Acknowledgment: NIH grants RO1 AR49553, RO1 AR50068